Graphene oxide doped polysulfone membrane adsorbers for the removal of organic contaminants from water

Massimo Zambianchi,[a] Margherita Durso,[a] Andrea Liscio,[a,b] Emanuele Treossi,[a] Cristian Bettini,[a] Massimo L. Capobianco,[a] Annalisa Aluigi,[a] Alessandro Kovtun,[a] Giampiero Ruani,[c] Franco Corticelli,[d] Marco Brucale,[c] Vincenzo Palermo,[a,] Maria Luisa Navacchia,[a,*] Manuela Melucci[a,*]*

[a] Consiglio Nazionale delle Ricerche, Istituto per la Sintesi Organica e la Fotoreattività, (CNR-ISOF), via P. Gobetti 101, 40129 Bologna, Italy

[b] Consiglio Nazionale delle Ricerche, Istituto dei Sistemi Complessi, (CNR-ISC), via del Fosso del Cavaliere 100, 00133 Roma, Italy

[c] Consiglio Nazionale delle Ricerche, Istituto per lo Studio dei Materiali Nanostrutturati (CNR-ISMN), via P. Gobetti 101, 40129 Bologna, Italy

[d] Consiglio Nazionale delle Ricerche, Istituto per la Microelettronica e i Microsistemi (CNR-IMM), via Gobetti 101 - 40129 Bologna, Italy

Corresponding authors emails: marialuisa.navacchia@isof.cnr.it, vincenzo.palermo@isof.cnr.it, manuela.melucci@isof.cnr.it.

Keywords. graphene oxide, polysulfone, membrane adsorbers, organic contaminants removal.

ABSTRACT

This work explored polysulfone (PS)- graphene oxide (GO) based porous membranes (PS-GO) as adsorbent of seven selected organic contaminants of emerging concern (EOCs) including pharmaceuticals, personal care products, a dye and a surfactant from water. PS-GO was prepared by phase inversion method starting from a PS and GO (5% w/w mixture). The porous PS-GO membranes showed asymmetric and highly porous micrometer sized pores on membrane top (diameter ≈20 μm) and bottom (diameter ≈ 2-5 μm) surfaces and tens of microns length finger like pores in the section. Nanomechanical mapping reveals patches of a stiffer material with Young modules comprised in the range 15-25 GPa, not present in PS pure membranes that are compatible with the presence of GO flakes on the membrane surfaces. PS-GO was immersed in EOCs spiked tap water and the adsorbance efficiency in time and at different pH evaluated by HPLC analyisis. Ofloxacin (OFLOX), Benzophenone-3 (BP-3), rhodamine b (Rh), DCF and triton X-100 (TRX) were removed with efficiency higher than 90% after 4 hours treatments. Regeneration of PS-GO and reuse possibilities were demonstrated by washing with ethanol. The adsorption efficiency toward were

Moreover, PS-GO outperformed a commercial granular activated carbon (GAC) at low contact times and compared well at longer contact time for OFLOX, Rh, BP-3 and TRX suggesting the suitability of the newly introduced material for drinking water treatment.

1. Introduction

The number of new organic compounds entering every year the global market is growing tremendously. Most of these compounds, including pharmaceuticals, personal care products, pesticides and surfactants are worldwide used in large quantities in human and industrial activities and after use are disposed in different water compartments where they can persist causing severe environmental and health problems. Indeed, due to the huge variety of these pollutants, the conventional wastewater treatment plants are not always effective. [1] Consequently, the number of cases of contamination of ground and even drinking water is rapidly increasing throughout the world, and is matter of great environmental concern. [2] Advanced oxidation processes (AOP) have demonstrated high effectiveness for their removal of several endocrine disrupting compounds (EDCs) including pesticides, halogenated and aromatic compounds compounds and alkylphenols. However, the costs of these processes are high because of the electric energy consumption when UV radiation is applied. [3]

Adsorption on Granular Activated Carbon (GAC) is the most common approach to remove organic contaminants from water. Activated carbon adsorption has been cited by the US Environmental Protection Agency as one of the best available control technologies for the removal of organic dyes. [4] GAC have also proven to be a good adsorbant for different type of pharmaceuticals [5] However, the costs associated with their regeneration (i.e. off-site transport, thermal treatments and material lost during these processes), [6] combined to a decrease of the adsorption capability with time after regeneration , [7] encourage the search for novel alternative adsorbant materials.[8]

Graphene oxide (fig. 1a), due to its high surface area, high dispersibility in water combined to the low production costs, is attracting increasing interest as new adsorbant for

environmental applications. [9] GO can adsorbs several organic species by means of π- π interactions, electrostatic interactions or also ion exchange.[10] Recently, GO nanosheets have been exploited for the removal of aromatic contaminants such as biphenyl based foams have been used to remove diesel, [11] gasoline, motor oil and petroleum [12] as well as organic dyes from wastewater. [13-18]

Polysulfone (PS, fig. 1a) is a thermally stable, biocompatible and super hydrophobic polymer that can be processed into mechanically strong porous ultrafiltration membranes of wide use for haemodialysis and water microbiologic depuration industrial fields. The addition of nanomaterials such as silica nanoparticles [19] carbon nanotubes [20] or modified graphene oxide [21] to PS membranes, has been recently proposed to enhance their range of applications for example to the filtration of oil residues removal from wastewater. [22] Rezaee et al. [23] recently reported the fabrication of GO doped polysulfone membranes (0.5-2% w/w of GO) and its successful use for the removal of arsenate from water by filtration. Here, we demonstrate for the first time the possibility to exploit GO doped polysulfone composite membranes as adsorbers for several classes of organic compounds from water including molecules of emerging environmental concern (EOCs).

The membranes were fabricated by phase inversion method and the amount of GO (5% w/w) tailored to maximize the effect of GO on the final adsorption capability and selectivity of the composite (PS-GO).

A mixture of seven organic compounds of emerging concern belonging to pharmaceuticals, pigments, personal care products and surfactants in water was considered for our investigation (fig. 1b). The rational for the choice relies on the following reasons: i) the selected compounds are of main environmental concern, for example diclofenac (DCF), [24] is the most diffused

non-steroidal anti-inflammatory drug and has been recently included by the European Commission in the new priority hazardous substances list (Directive 2013/39/UE)[25]; ii) collectively these compounds are representative of a variety of chemical functional groups such as condensed aromatic rings, carboxylic/sulfonic acid, zwitter ions, that can be useful to shed light on the removal mechanism[26]; iii) a greater toxicological effect for pharmaceuticals in mixture rather than individually at the same concentration has been observed.[27]

Figure 1. a) Simplified chemical structure of PS and GO; b) molecular structures, acronyms and class of the target organic compounds herein considered.

2. Materials and methods

2.1. Chemicals and stock solutions

OFLOX, CBZ, DCF, BP-3, BP-4, TRX, Rh polysulfone pellets (PS, average M_W 35.000), *N*-methyl-2-pyrrolidone (NMP) and LC-MS grade acetonitrile were purchased from Sigma-Aldrich in the highest available purity and were used without any further purification. GAC-coal based UltraCarboBios (for water fish tanks depuration), in pellets (BET Surface area 800±60 m^2/g, apparent density 500 kg/m^3, diameter 3 mm, length 5-10 mm) were employed. Ultrapure deionized water (resistivity 18.2 MΩ/cm at 25 °C) was produced in our laboratory by means of a Millipore Milli-Q system. Tap water was collected from municipal waterworks of Bologna (conductivity 470 μS/cm).

EOCs stock solution (1 L) of 5.0 mg of each analyte was prepared in tap water. In order to ensure complete dissolution of the analytes the stock solution was stirred for 48 hs and kept in the dark due to the presence of light sensitive compounds. The pH was monitored during the experiments (fig. S7).

The EOCs solutions at pH 3. and pH 9.0 were prepared by addition of HCl 6N (200 μl) or of NaOH 1M (400 μl), respectively, to 1 L of EOC solution in milliQ water.

2.2. Membranes preparation

PS-GO membranes (5% wt/wt of GO) were prepared by phase inversion method [28]. GO (50 mg, prepared by unmodified Hummers method) was dissolved in *N*-methyl-2-pyrrolidinone (5 g) and sonicated for 16 hs at room temperature. After addition of polysulfone pellets (1 g), the mixture was heated at 60°C for 1 h until complete dissolution of PS, then cooled to room temperature. Aliquots of 500 mg of the resulting black solution, were pipetted into different glass vials (25 mm diameter). After a 30-sec exposure period in a controlled environment (air at 22°C and 60% relative humidity), the vials were gently immersed in deionized water to induce porous membrane formation. After detachment from the vials, the PS-GO membranes were washed overnight with fresh water and finally dried at 50°C to a constant weight. PS-GO membranes of total weight ≈85 mg, diameter 25 mm were obtained. The membranes were cut into small pieces and used in a total weight of 50 mg for the adsorption experiments.

PS membranes (fig. S1) were prepared from a casting solution of PS (17 w%) in NMP at 60°C [28]. PS membranes of total weight ≈85, diameter 25 mm were obtained. As for PS-GO, the membranes were cut into small pieces and used in a total weight of 50 mg for the adsorption experiments.

2.3. Characterization techniques

SEM was performed by using Environmental Scanning Electron Microscope Zeiss EVO LS 10 LaB6. Attenuated Total Reflectance Fourier Transform (ATR FT-IR) measurements were performed with a N_2 purged Bruker Vertex 70 interferometer using a single reflection Platinum-ATR accessory (diamond crystal), a DLaTGS detector and a KBr beamsplitter. Micro-Raman spectra were recorded by using a Renishaw micro-Raman 1000 system exciting at 632.8nm (HeNe laser). The laser beam was focused through a x50 objective. To avoid local heating of the film in the laser spot during the measurement, laser power density was kept below 1KW/cm^2. The mechanical characterization was performed on a Multimode 8 AFM microscope equipped with a Nanoscope V controller and type E and J piezoelectric scanners (Bruker, USA) via the PeakForce Quantitative Nanomechanical Mapping (QNM) module, employing TESP and TAP525 probes (Bruker, USA). The N_2 adsorption and desorption isotherms were measured using the ASAP 2020 analyser (Micromeritics, USA). Before the N_2 isothermal analysis the membranes were pre-treated at 50° C for 4 h under vacuum until the pressure was equilibrated to 10^{-5} Torr. The surface area was measured by using multi-point adsorption data from linear segment of the N_2 adsorption isotherms using Brunauer-Emmett-Teller (BET) theory in according with ASTM D6556 – 10[CIT, ASTM D6556 – 10, Standard Test Method for Carbon Black-Total and External Surface Area by Nitrogen Adsorption].

pH measurements were performed by a Delta OHM, HD8602 pH meter.

2.4. Adsorption experiments

In a typical experiment PS-GO (total weight of 50 mg) is immersed in the EOCs solution (4 ml) in tap water and stirred with a magnetic bar (1 cm length) at room temperature.

For the comparative experiments with PS, GO and GAC we used GO (2.5 mg corresponding to the amount of GO present in PS-GO), PS (50 mg) and for GAC (50 mg). The sample tests, as well as the reference original solution, were kept in darkness.

2.5. Reuse and regeneration experiments

PS-GO membrane (50 mg) was immersed in a stirred EOC solution (4 ml, 5mg/L of each) and after 4hs the membrane was removed and immersed in ethanol (EtOH) for 30 minutes. After quick drying with N_2, the membrane was immersed in a fresh EOC solution (4 ml, 5mg/L of each) and the removal efficiency measured after 4hs. Three cycles of regeneration-reuse experiments were performed (see fig. 8). A total volume of 3 ml of EtOH was used.

2.6. Analytical determination in solutions

High-performance liquid chromatography coupled with a variable wavelength detector (Agilent Technologies, 1260 Infinity) and a Varian Pro Star fluorescence detector was used for quantification of the analytes at different treatment times. The chromatographic separation was performed following a method specifically developed for this application using a C-8 analytical column (Agilent XDB-C8, 4.6×50 mm^2, see table S1). Aliquots of 40 μL were injected. No filtration was necessary prior to the injection. Only in the case of the experiments with GO and GAC centrifugation of the samples at 8000 RPM for 5 min was necessary prior to the HPLC analysis. UV signal was recorded at different wavelengths according to the wavelength of maximum light absorption of OFLOX, BP-4, CBZ, DCF and BP-3. In the case of TRX the fluorescent emission peak was used for the detection (details in table S2). The response limit of detection (LOD) for each analyte was established as the first lowest calibration point of the calibration curve (linear regression, $R^2 > 0.99$, details in electronic supplementary material), i.e. 50 μg/L. All injections were repeated 3 times and the average

values were used for calculations of the percentage of removal (see table S3 and S4). The analytical samples were kept in amber glass vials and analyzed at earliest convenience. Besides, for each sample, an untreated EOCs solution was analyzed as reference at the chosen intervals of time.

3. Results and Discussion

3.1. PS-GO membranes fabrications and characterization

PS-GO was prepared by phase inversion method [28] as described in the experimental part. The amount of GO was the highest that enabled stable and good dispersibility in NMP and that allow complete inglobation of GO in the PS matrix during the composite precipitation. At higher amount, indeed part of GO was dispersed in water during the phase inversion.

Figure 2. a) Image of a cut PS-GO membrane. b) ESEM image of the section of the membrane (top layer is also visible) c) detail of the membrane top skin, d-e) detail of the porosity at different magnification, f) inner porous layer at the bottom skin layer side. The image of a PS pure membrane is reported for comparison (Figs. S1, S2).

The structure of PS-GO (as prepared membrane in fig. 2a) as observed by ESEM features a highly porous, asymmetric 3D structure (figure 2b). One of the outer skin is dense with a underlayer made of finger like pores tens of microns length and a few microns large (fig. 2c). As observed by Rezaee et al. [23] in membranes with lower amount of GO (max 2% wt/wt), the addition GO on the PS membrane morphology results in larger pore size and formation of macrovoids in the finger like pores sublayer (fig. 2c, figs. S1,S2).

Below this layer a thick layers with a hierarchical porous structure was observed (figs. 2d,e, fig. S1). The inner pores show maximum diameter of about 20 μm with a finer nanoscale

structure, i.e. pores with size <<1μm (fig. 2e). The opposite skin layer (fig. 2s bottom) show homogeneously distributed pores few microns sized (2-5 μm).

Comparative FTIR-ATR and Raman spectroscopies performed on PS, GO and PS-GO confirm the simultaneous presence of both PS and GO components. ATR spectra (fig. 3a) show almost overlapping PS and PS-GO spectra, while the Raman spectra (fig. 3b) confirm the presence of GO in both the top and the bottom surface of PS-GO. The morphometric and nanomechanical surface characteristics of PS and PS-GO were characterized via Atomic Force Quantitative Nanomechanical Mapping (AFM-QNM). The morphological micrographs of PS and PS-GO show abundant micron-sized cavities and amorphous globular accretions (fig. 4, left column). Due to the random distribution of these features, area roughness parameter Sq has a very large variance when measured at the μm^2 scale. However, Sq values measured on the flatter regions of the samples (i.e. by excluding cavities and accretions from the calculation) have a comparatively small variance and are remarkably similar for PS (45±9 nm) and PS-GO (56±12 nm) at the μm^2 scale.

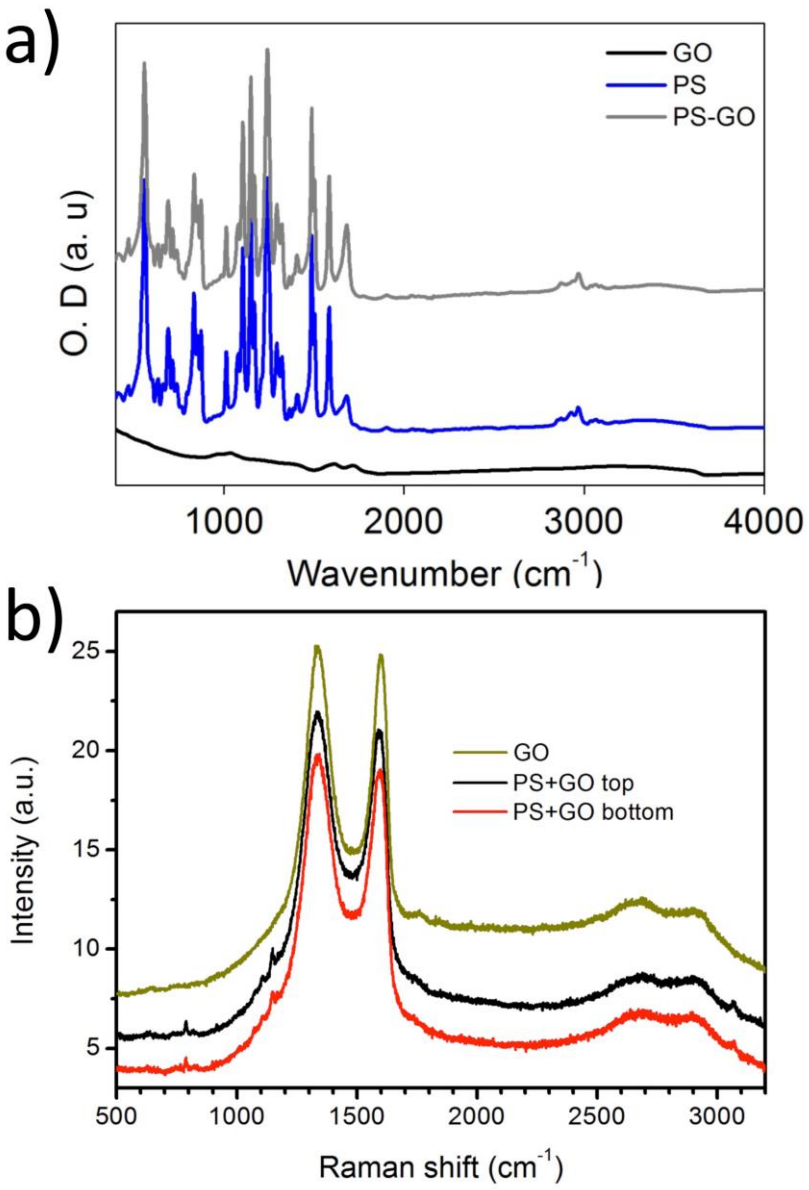

Figure 3. a) ATR and b) Raman (λexc = 633nm) spectra of GO, PS and PS-GO samples (top and bottom membrane surface).

Exerting a local force of 150 pN on the samples resulted in an average measured elastic deformation of 8.5±0.1 nm (PS) and 6.2±0.2 nm (PS-GO), thus justifying the use of a cone-to-surface (Sneddon) contact mechanics model for subsequent calculations since the tip curvature radii were estimated to be in the range of 2-3 nm. The resulting Young Modulus

maps (figure 4, right column) yield an average modulus of E = 2.4±0.1 GPa for bare PS, in good agreement with bulk measurements [29], with local values reaching at most ~10 GPa in correspondence of steep topographical features, thus suggesting that the observed variations are transient artifacts due to the geometry of tip-surface interaction. In contrast, PS-GO was measured to have an average E of 5.9±0.6 GPa, with extended continuous zones of stiffer material with E up to ~50 GPa (see fig. 4).

It is noteworthy to underline that the position of these zones was found to be uncorrelated with topographical features, thus excluding the possibility of artifacts causing the signals, and suggesting the incorporation of stiffer material inside the PS matrix.

The modulus values of the harder regions were found to be mostly comprised in the range of 15-25 GPa, which is at least one order of magnitude lower than any experimentally measured E value of single GO flakes subjected to different types of uniaxial stress (~0.2-1.0 TPa). [29-33]

However, the apparent discrepancy is easily reconciled if considering that in PS-GO the GO flakes are resting on, and covered with, a softer material.

Nitrogen adsorption and desorption curves of PS-GO and PS were also performed (figure S3). Almost identical, BET surface area were found with values of 3,1 ± 0,3m^2/g and 3,4 ± 0,3 m^2/g for PS and PS-GO respetively, confirming that GO does not affect the adorption properties of the PS membrane.

Figure 4. Representative AFM morphology (left column) and corresponding Young Modulus (right column) micrographs of PS (top) and PS-GO (bottom). All scale bars are 1μM. The nanomechanical mapping of PS-GO reveals patches of stiffer material, the position of which is uncorrelated with topography. These harder regions are absent in PS pure membranes.

3.2. Adsorption efficiency, mechanism and comparison to GO, PS and GAC

The efficiency of PS-GO in the removal of the target organic compounds in mixture was investigated by immersing PS-GO in the contaminated water and estimating by HPLC the amount of organic molecules removed after stirring at room temperature for several hours. Figure 5 shows the images of vials containing the adsorbents immersed in the organic solution mixture during the treatment at different contact time. Differences in the color of the solution after treatment can be clearly seen even by eye, with a lighter pink color for PS-GO and GO samples with respect to PS.

The selectivity and removal efficiencies of PS-GO at different pH are displayed in fig. 6. PS-GO showed an almost quantitative removal for OFLOX, Rh, BP-3 and TRX, while lower affinity was observed for the other compounds (details in table S3, ESI).

Figure 5. Capture of the target molecules in mixture (the pink color is due to the Rh dye) by PS-GO, GO and PS. Discoloration of the solution over time is due to the removal of the Rh.

Fig. 6a shows that on passing from 1h to 4hs, the removal efficiency increased significantly for almost all compounds, while a less marked effect was observed on increasing the contact time from 4hs to 24hs. Therefore, we choose the value of 4 hs being the best compromise between treatment time and removal efficiency. Similar results were found at lower initial concentrations (0.5 mg/L of each compound, see table S4) indicating that the adsorbent performance is not significantly affected by the concentration in the investigated range (0.5-5

mg/L of each compound). No difference in PS-GO performances were found in both tap and milliQ water (see fig. S4, ESI) indicating that the background of tap water does not interfere with the adsorption on PS-GO, this suggesting possible exploitation for drinking water treatment.

The performance of PS-GO was poorly affected by pH, as shown in fig S6, this highlighting that PS-GO can work in a wide range of pH. Interestingly, in the case of DCF a significant removal enhancement (19 → 85%) was found at pH 3. Similar trend on DCF was found also for pure PS and GO (see table S5a, ESI), suggesting that the pH induced removal enhancement is mainly related to the chemical species rather than to the adsorbent. Indeed tha carboxylic acid of DCF having pKa=4, at pH 3 is in the associated form (pKa 4) for which different chemo-physical properties can be expected.[34]

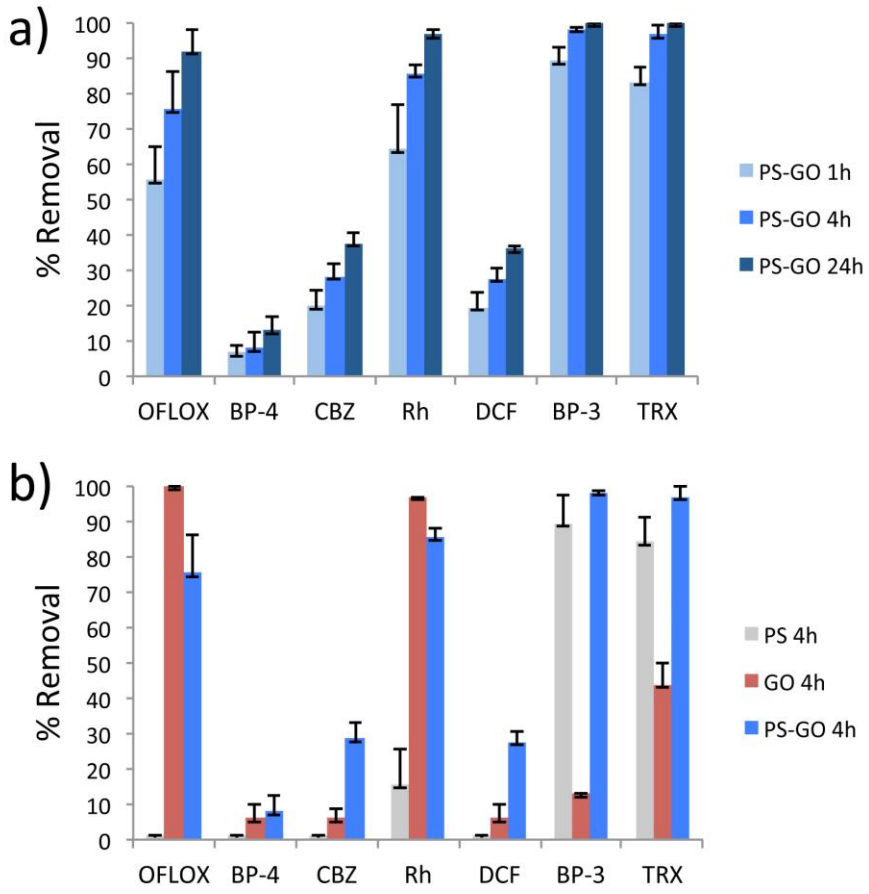

Figure 6. Effect of a) contact time and b) Comparison between PS-GO, PS and GO (4hs, pH about 7 see fig. S7). Experiments at 5 mg/L of each EOCs perfomed in triplicates.

Figure 6b shows the comparison of selectivity and efficiency between PS-GO and pure PS and GO. PS and GO showed markedly different selectivity properties, which are efficiently combined in PS-GO. For instance, OFLOX poorly removed by PS but quantitatively removed by GO, is efficiently removed by PS-GO. On the other hand, BP-3 that is well removed by PS and poorly removed by GO, is removed by PS-GO with efficiency higher than 90%. Nevertheless, in the cases of DCF and CBZ, not removed by PS and poorly removed by GO (<10%) a significant enhancement of efficiency was found for PS-GO.

3.3 Comparison with commercial GAC

The performance of PS-GO was also compared to that of a commercial GAC sample. Figs. 7a shows that at 1h contact time, PS-GO outperforms GAC in particular in the removal of OFLOX, Rh, BP-3 and TRX. On these compounds, PS-GO at 4hs still outperforms GAC whereas for BP-4, CBZ and DCF, GAC showed higher efficiencies. At longer contact time (24hs, fig. 7c) the same trend is observed, with almost comparable performances on OFLOX, Rh, BP-3 and TRX and highest performance for GAC on BP-4, CBZ and DCF.

A possible explanation for the highest performances of GAC on BP-4, CBZ and DCF that can rely on their lower polarity and hydrophilicity with respect to the other compounds (see discussion below).

The faster removal rate of PS-GO respect to GAC could be due to the hierarchical, complex structure of the material at multiscale. The presence of large pores at the macroscale and the GO polarity facilitate the solution penetration, while the smaller ones at the microscale combined to the GO sheets presence provide to increase the effective surface area available for adsorption.

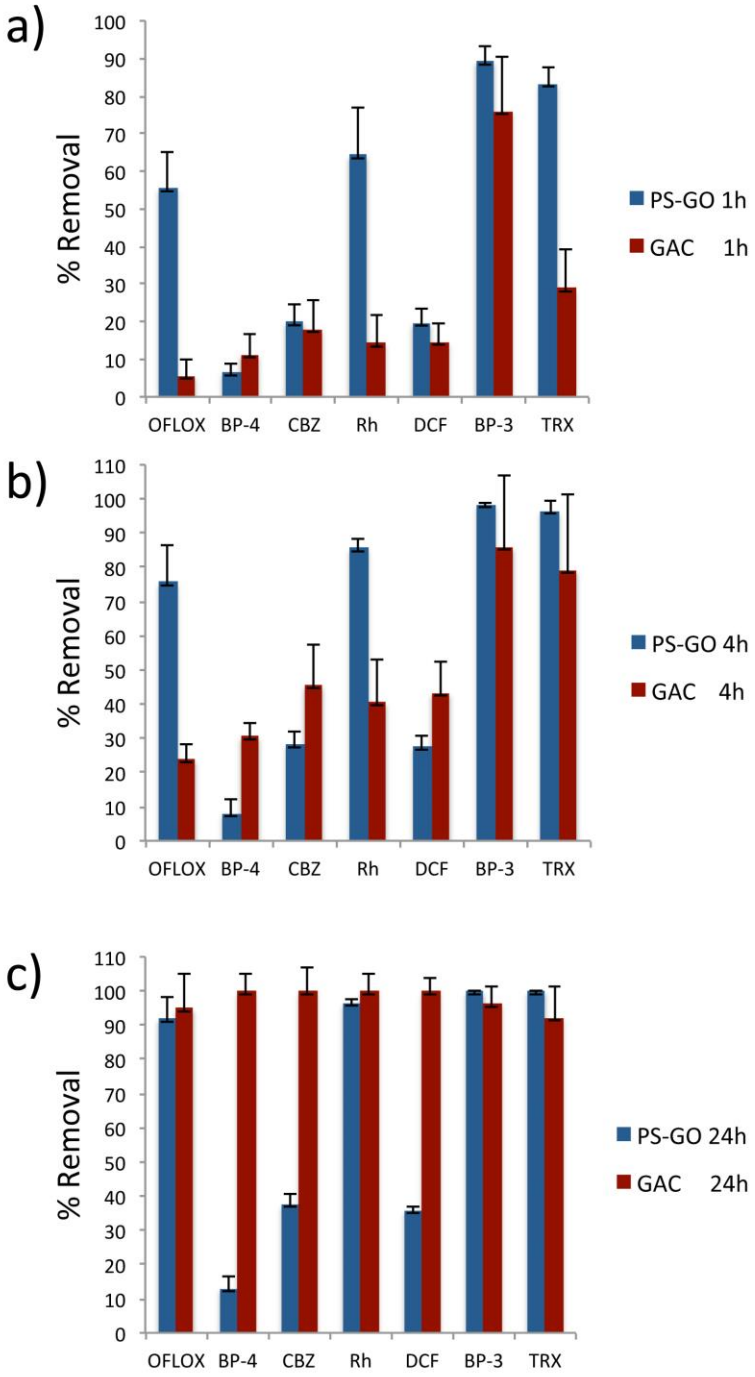

Figure 7. Removal efficiency of PS-GO (50 mg) and GAC (50 mg) at different time (5 mg/L of each EOC).

3.4 Reusability and regeneration

The possibility of regenerate and reuse PS-GO membranes was investigated by using the same membrane in consecutive adsorption experiments after regeneration by washing with small amount of ethanol (see experimental details) that in our optimized conditions does not dissolve neither polysulfone nor graphene oxide but is a good solvent for organic compounds.

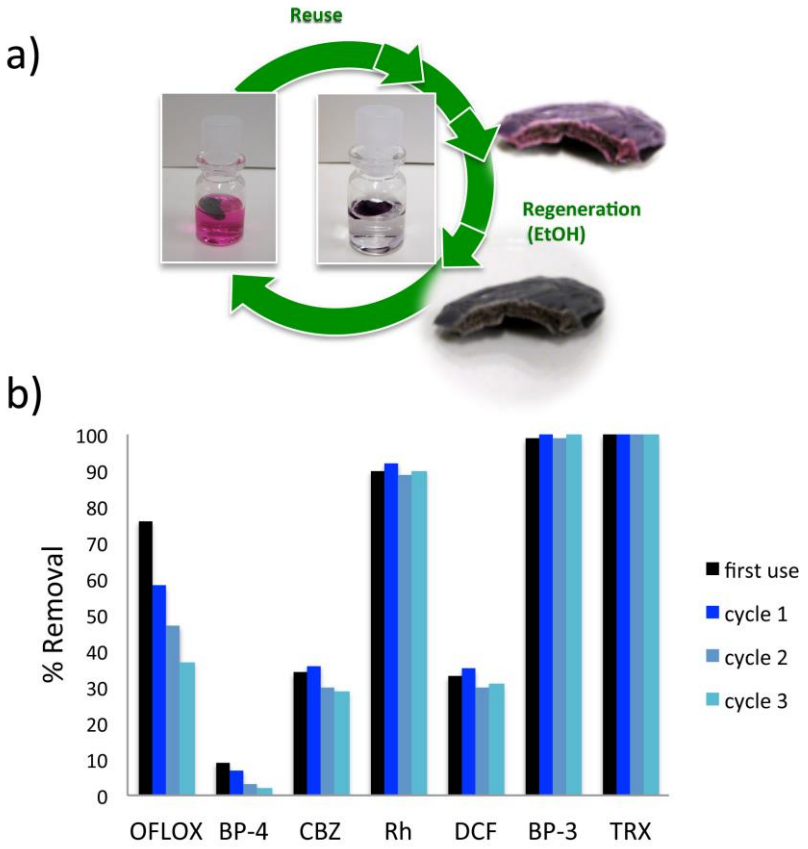

Figure 8. Sketch of the regeneration process and b) performance of a PS-GO membrane after concecutive regeneration-reuse cycles (EOCs 5 mg/L each, contact time 4hs)..

Figure 8 shows that the removal percentage after each cycle, even after regeneration are almost comparable. Only in the case of ofloxacin a drop of removal efficiency of about 30% was observed. A possible explanation relies….

3.5 Adsorption mechanism

To have an insight on the adsorption mechanism we analysed the removal efficiency as a function of the solubility, hydrophilicity and polarity of the targeted organic compounds (table 1). Our data suggest that hydrophilicity and polarity play a crucial role on the adsorption efficiency of GO and of PS-GO. Indeed, GO removed with higher efficiencies highly polar molecules such as OFLOX and Rh (13 and 25 Debye respectively) and was less efficient on less polar CBZ (2,4 Debye) and DCF (1 Debye). On the contrary, solubility does not influence significantly the removal efficiency. As shown by data on OFLOX and BP-4 having similar water solubility (28300 mg/L, 20000 mg/L respectively) are adsorbed with markedly different efficiency (100% and 13% respectively).

Polysulfone PS, adsorbed efficiently only TRX and BP3 and RhB at lower extent. In this case, less clear were the relationships between molecular structure and adsorption behaviour. For example, BP3 similar to CBZ in terms of solubility, polarity and hydrophilicity, was efficiently adsorbed, while CBZ was not adsorbed at all. Nevertheless, data on DCF at pH 3, at which DCF carboxilyc acid is protoned (pKa=4), i.e. less hydrophilic indicate that higher hydrophobicity improves the adsorbance on PS. A similar behaviour was found for PS on the adsorption of ofloxacin having a carboxylic substituents (pKa 5,45) that was negligible at pH7 and increases up to about 30% at pH3 (table 5b SI).

Table 1. Summary of some chemophysical parameters of the selected EOC.

	BP-3	CBZ	DCF	BP-4	OFLOX	Rh	TRX
Log Kow	3,79	2,5	4,5	0,4	-0,4	-1,1	/
Dipole moment (Debye)	/	2,4	1,0	/	13,0	25,0	/
Water Solubility (mg/L)	69	112	2425	20000	28300	34000	100000

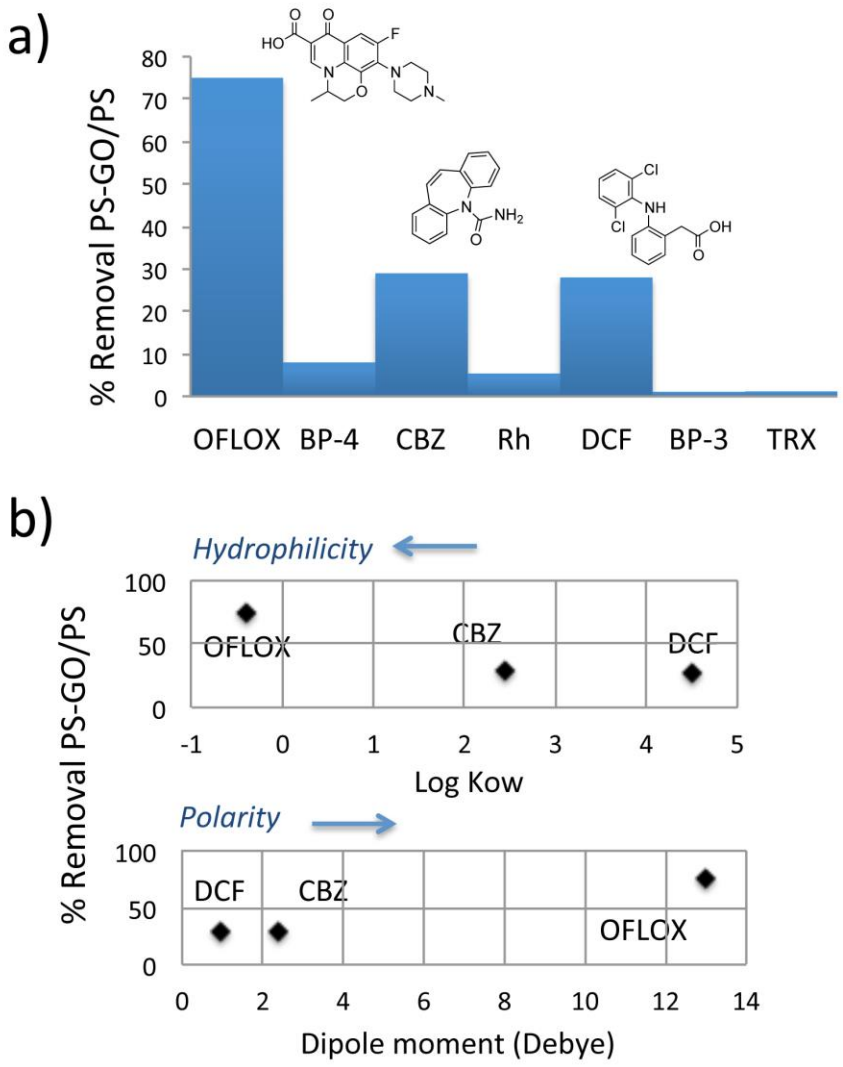

Figure 9. a) Improvement of the removal of PS-GO respect to PS only material (PS-GO/PS) for each compound. The improvement is calculated as the ratio between the removal of PS-GO and that of PS (data in table S6, ESI). b) trend between the removal efficiency improvement PS-GO/PS and hydrophilicity and polarity of OFLOX CBZ and DCF.

PS-GO adsorption behavior was mainly determined by GO as clearly showed by the analysis of the removal efficiency improvement of PS-GO with respect to pure PS membranes (fig. 9a) versus the hydrophilicity and dipole moment of the target organic molecules (PS-GO/PS). The highest improvement values were observed for OFLOX, CBZ and DCF (fig. 9a). A linear

trend between the improvement values and the hydrophilicity and polarity was observed. In turn, the highest removal improvement (PS-GO/PS) was found for the most hydrophilic and polar compound (OFLOX), indicating that the addition of even a small amount of GO to PS, strongly favors the adsorbance of hydrophilic and polar molecules. A further possible explanation could relies on a higher surface wettability of PS-GO promoted by the presence of GO [23] that increase the water permeability through the composite.

The adsorption isotherm study -----[35-36 ref da dedicare a isoterme]

Table 2. Adsorption Isotherm parameters

Model	Parameters	Rhodamine	Ofloxacin
Langmuir $q = q_{max} \times \frac{K_L C_e}{1 + K_L C_e}$	q_{max} (mg/mg) K_L (mL/mg) R^2	0,02983 0,12207 0,93201	0,0038 58,8 0,98252
Freundlich $q = K_f C_e^{1/n}$	k_f (mg/mg)(mL/mg)$^{1/n}$ n R^2	0,00334 1,3 0,94153	0,00411 6,71 0,75939
Dubinin-Radushkevich $lnq = lnq_{max} - k\varepsilon^2$	q_{max} (mol/mg) E (kJ/mol) R^2	5,7856E-08 21,6 0,66467	3,7562E-08 29,1 0,89198
BET $q_e = \frac{K_B \cdot C_e \cdot q^0}{(C_S - C_e) \cdot [1 + (K_B - 1)(C_e/C_S)]}$	q^0 (mg/mg) K_B (ml/mg) C_s (mg/ml) R^2	0,00200 ≈ 100 4,8	nd

Maximum adsorption capability around xx mg of Rh for gram of adsorbent was found. This result compares well to other adsorbent already reported in literature, which are mainly based on activated carbons. Indeed maximum Rh absorption capability in the range from few mg/g to hundreds of mg/g was reported for activated carbons derived from biological origin (i.e. palm or coconut shell). [37, 38] Highest capacity were estimated for spherical activated

carbons (about 1000 mg/g). [39] On the other hand, maximum absorption capability in the range of 10-50 mg/g, as for PS-GO was reported for other graphene oxide hybrids. [9, 40]

On the other hand, for ofloxacin maximum adsorption capability around xx were found. For this compound adsorption efficiency in the range 25-40 mg/g were reached by using cork (M. Crespo-Alonso, V. M. Nurchi, R. Biesuz , G. Alberti, N. Spano, M. I. Pilo, G. Sanna *Biomass against emerging pollution in wastewater: Ability of cork for the removal of ofloxacin from aqueous solutions at different pH* Journal of Environmental Chemical Engineering 1 (2013) 1199–1204).

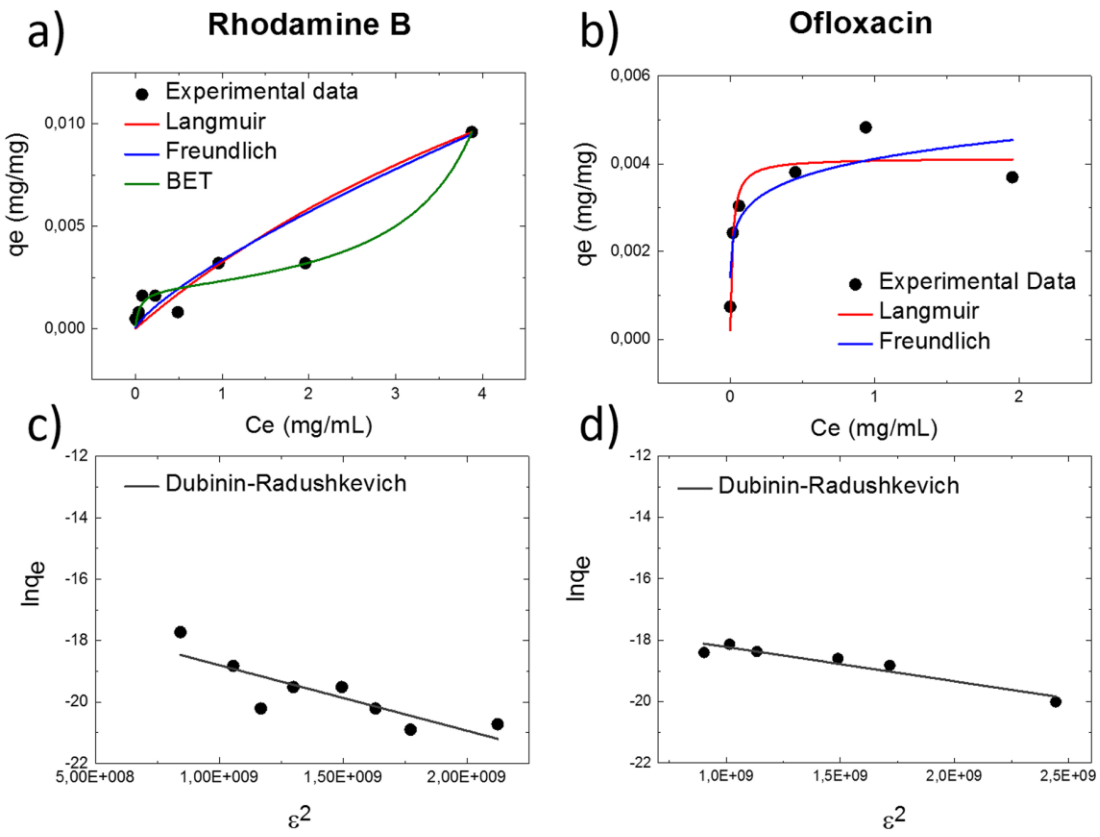

Figure 10. Plots of the fitting of the experimental data with Langmuir, Freundlich, BET and Dubinin-Radushkevich, for rhodamine and ofloxacin. Adsorption isotherm at 20°C, pH 7,

contact time 24 hours (50 mg of adsorbent PS-GO, volume 4 ml, C_0 4-0.01 mg/ml for rhodamine and 2-0,01 mg/ml for ofloxacin.

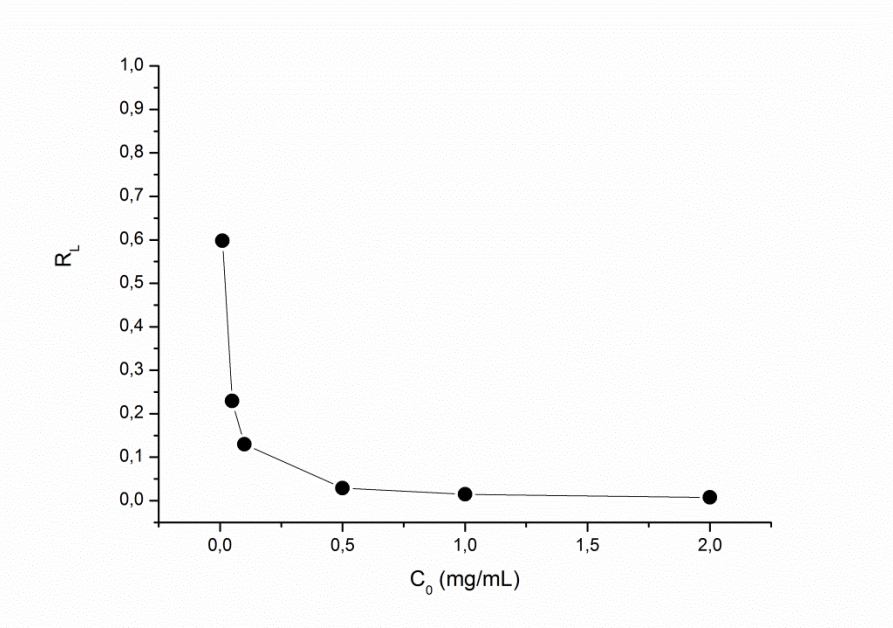

Figure 11. Separation factor for the adsorption of ofloxacin on PS-GO.

4. Conclusions

In conclusions, we have reported the preparation and characterization of a GO doped PS porous membrane and its use as adsorber for seven selected organic compounds of environmental relevance. PS-GO shows high affinity for the majority of the targeted organic compounds with GO-driven preferential adsorption of hydrophilic and polar molecules and can work in a wide range of pH (3-9) with a significant improvement for the removal of DCF at pH 3. Improved performance with respect to pure PS and GO, in particular for CBZ and DCF were found for PS-GO. Moreover, PS-GO at low contact time is competitive with commercial GAC and compares well at longer contact time for OFLOX, Rh, BP-3 and TRX this encouraging further engineering of PS-GO adsorbers. The use of GO based composites for organic compounds removal has been so far limited to a few targets, mainly organic dyes

and small aromatics. [9, 40] Moreover, in previous study addition of small amount of graphene-oxide to polysulfone membranes has been exploited to enhance the hydrophilicity, mechanical stability and fouling resistance of polysulfone membranes.

Our work demonstrates for the first time that the addition of GO to polysulfone membranes promotes adsorption properties toward polar hydrophilic organic compounds. Membrane filtration and adsorption are generally considered two separate functionalities but we demonstrate that PS membranes - commonly exploited for filtration- can be tailored to work also as adsorbant opening the way to the development of tailored PS and GO based materials for specific water treatments.

Acknowledgements

The research leading to these results has received funding from the European Union Seventh Framework Programme under grant agreement n°604391 Graphene Flagship, the EC Marie-Curie ITN- iSwitch (GA no. 642196). MM thanks Dr. Alessandro Kovtun for the BET analysis.

Appendix A. Supplementary data

The following supplementary data related to this article are available on line. . HPLC method details, Scanning Electron Microscopy of PS-GO and PS only membrane, N2 adsorption/desorption curves, Water contact angle, Calibration curves, Removal data of a typical experiment at two different concentration, Comparison between tap water and milliQ water, Effect of pH for PS-GO, PS and GO, pH monitoring during the adsorption experiments.

.

References

[1] B. Petrie, R. Barden, B. Kasprzyk-Hordern, A review on emerging contaminants in wastewaters and the environment: current knowledge, understudied areas and recommendations for future monitoring, Water Research 72 (2015) 3-27.

[2] (a) G. A. Loraine, M. E. Pettigrove, Seasonal variations in concentrations of pharmaceuticals and personal care products in drinking water and reclaimed wastewater in southern California, Environ. Sci. Technol. 40 (2006) 687-695;

(b) J. Gibs, P. E. Stackelberg, E. T. Furlong, M. Meyer, S. D. Zaugg, R. L. Lippincott, Persistence of pharmaceuticals and other organic compounds in chlorinated drinking water as a function of time, Sci. Total Environ. 373 (2007) 240-249;

(c) R. Rodil, J. B. Quintana, E. Concha-Grana, P. Lopez-Mahia, S. Muniategui-Lorenzo, D. Prada-Rodriguez, Emerging pollutants in sewage, surface and drinking water in Galicia (NW Spain), Chemosphere 86 (2012) 1040-1049.

[3] M. Gmurek, M. Olak-Kucharczyk, S. Ledakowicz, Photochemical decomposition of endocrine disrupting compounds – A review, Chem. Eng. J. 310 (2017) 437-456.

[4] Derbyshire, F., Jagtoyen, M., Andrews, R., Rao, A., Martin-Gullon, I., Grulke, E., 2001. Carbon materials in environmental applications. In: Radovic, L.R. (Ed.), Chemistry and Physics of Carbon, Vol. 27. Marcel Dekker, New York, pp. 1–66.

[5] (a) Z. Yu, S. Peldszus, P.M. Huck, Adsorption characteristics of selected pharmaceuticals and an endocrine disrupting compound-Naproxen, carbamazepine and nonylphenol-on activated carbon, Water Research 42 (2008) 2873-2882;

(b) E. S. Rigobello, D. A. Di Bernardo, L. Di Bernardo, E. M. Vieira, Removal of diclofenac by conventional drinking water treatment processes and granular activated carbon filtration, Chemosphere 92 (2013) 184-191;

(c) A. Katsigiannis, C. Noutsopoulos, J. Mantziaras, M. Gioldasi, Removal of emerging pollutants through Granular Activated Carbon, Chem. Eng. J. 280 (2015) 49–57.

[6] Dabrowski, A., 2001, Adsorption from theory to practice, Advances in Colloid and Interface Science 93, 135-224 .

[7] A. Matilainen, N. Vieno, T. Tuhkanen, Efficiency of the activated carbon filtration in the natural organic matter removal, Environment International, 32 (2006) 24-331.

[8] (a) G. Crini, Non-conventional low-cost adsorbents for dye removal: A review, Bioresource Technology 97 (2006) 1061–1085;

(b) I. Ali, V. K. Gupta, Advances in water treatment by adsorption technology, Nature Protocols 1 (2007) 2661-2667.

[9] (a) F. Perreault, A. Fonseca de Faria, M. Elimelech, Environmental applications of graphene-based nanomaterials, Chem. Soc. Rev. 44 (2015) 5861-5896;

(b) O. Suárez-Iglesias, S. Collado, P. Oulego, M. Díaz, Graphene-family nanomaterials in wastewater treatment plants, Chem. Eng. J. 313 (2017) 121–135;

(c) D. Shu, F. Feng, H. Han, Z. Ma, Prominent adsorption performance of amino-functionalized ultra-light graphene aerogel for methyl orange and amaranth, Chem. Eng. J. 324 (2017) 1–9;

(d) G. K. Ramesha, A. V. Kumara, H. B. Muralidhara, S. Sampath S. Graphene and graphene oxide as effective adsorbents toward anionic and cationic dyes, Journal of Colloid and Interface Science 361 (2011) 270–277.

[10] (a) W. Yu, S. Zhan, Z. Shen, Q. Zhou, D. Yang, Efficient removal mechanism for antibiotic resistance genes from aquatic environments by graphene oxide nanosheet, Chem. Eng. J. 313 (2017) 836–846;

(b) J. A. González, M. E. Villanueva, L. L. Piehl, G. J. Copello, Development of a chitin/graphene oxide hybrid composite for the removal of pollutant dyes: Adsorption and desorption study, Chemical Engineering Journal 280 (2015) 41–48.

[11] Apul, O.G., Wang, O., Zhou, Y., Karanfil, Y., 2013. Adsorption of aromatic organic contaminants by graphene nanosheets: Comparison with carbon nanotubes and activated carbon, Water Research, 47, 4648-1654.

[12] (a) H. Guo, T. Jiao, Z. Qingrui, G. Wenfeng, P. Qiuming, Y. Xuehai, Preparation of graphene oxide-based hydrogels as efficient dye adsorbents for wastewater treatment, Nanoscale Res. Lett. 10 (2015) 272-281;

(b) G. Z. Kyzas, E. A. Deliyanni, K. A. Matis, Graphene oxide and its application as an adsorbent for wastewater treatment, J. Chem. Technol. Biotechnol. 89 (2014) 196-205.

[13] Y. Wu, N. Yi, L. Huang, T. Zhang, S. Fang, H. Chang, N. Li, J. Oh, J. A. Lee, M. Kozlov, A. C. Chipara, H. Terrones, P. Xiao, G. Long, Y. Huang, F. Zhang, L. Zhang, X. Lepro, C. Haines, M. Dias Lima, N. Perea Lopez, L. P. Rajukumar, A. L. Elias, S. Feng, S. J. Kim, N. T. Narayanan, P. M. Ajayan, M. Terrones, A. Aliev, P. Chu, Z. Zhang, R. H. Baughman, Y. Chen, Three-dimensionally bonded spongy graphene material with super compressive elasticity and near-zero Poisson's ratio, Nature Commun. 6 (2015) 6141-6149.

[14] S. Barg, F. Perez, M., N. Ni, P. do Vale, R. C. Maher, E. Garcia-Tuñon, S. Eslava, S. Agboli, C. Mattevi, E. Saiz, Mesoscale assembly of chemically modified graphene into complex cellular networks, Nature Commun. 5 (2014) 4328-4337.

[15] H. Bi, X. Xie, K. Yin, Y. Zhou, S. Wan, L. He, F.mXu, F. Banhart, L. Sun, R. S. Ruoff, Spongy graphene as a highly efficient and recyclable sorbent for oils and organic solvents. Adv. Funct. Mater. 22 (2012) 4421-4425.

[16] Y. Zhao, C. Hu, Y. Hu, H. Cheng, G. Shi, L. Qu, Angew. Chem. Int. Ed., A versatile, ultralight, nitrogen-doped graphene framework, Angew. Chem. Int. Ed. 51 (2012) 11371-11375.

[17] M. Namvari, H. Namazi, Clicking graphene oxide and Fe_3O_4 nanoparticles together: an efficient adsorbent to remove dyes from aqueous solutions, Int. J. Environ. Sci. Technol. 11 (2014) 1527-1536.

[18] X. Wang, L. L. Lu, Z. L. Yu, X. W. Xu, Y. R. Zheng, S. H. Yu, Scalable template synthesis of resorcinol-formaldehyde/graphene oxide composite aerogels with tunable densities and mechanical properties. Angew. Chem. Int. Ed. 54 (2015) 2397-401.

[19] D. Sen, A. K. Ghosh, S. Majumder, R. C. Bindal, P. K. Tiwari, Sep. Purif. Technol., Novel polysulfone-spray-dried silica composite membrane for water purification: preparation, characterization and performance evaluation, Sep. Purif. Technol. 123 (2014) 79-86.

[20] S. Maphutha, K. Moothi, M. Meyyappan, S. E. Iyuke, A carbon nanotube-infused polysulfone membrane with polyvinyl alcohol layer for treating oil-containing waste water. Sci. Rep. 3 (2013) 1509.

[21] M. G. Kochameshki, A. Marjani, M. Mahmoudian, K. Farhadi, Grafting of diallyldimethylammonium chloride on graphene oxide by RAFT polymerization for modification of nanocomposite polysulfone membranes using in water treatment, Chem. Eng. J. 309 (2017) 206–221.

[22] (a) K. Goh, L. Setiawan, L. Wei, R. Si, A. G. Fane, R. Wang, Y. Chen, Preparation of graphene oxide-based hydrogels as efficient dye adsorbents for wastewater treatment. Nanoscale Res. Lett., 10 (2015) 272-281;

(b) K. Goh, L. Setiawan, L. Wei, R. Si, A. G. Fane, R. Wang, Y. Chen, Preparation, characterization and performance enhancement of polysulfone ultrafiltration membrane using PBI as hydrophilic modifier, J. Mem. Sci. 475 (2015) 1-8.

[23] R. Rezaee, S. Nasseri, A. H. Mahvi, R. Nabizadeh, S. A. Mousavi, A. Rashidi, A. Jafari, S. Nazmara, Fabrication and characterization of a polysulfone-graphene oxide nanocomposite membrane for arsenate rejection from water, J. Environ. Health Sci. Eng. 13 (2015) 61-71.

[24] (a) S. Wiegel, A. Aulinger, R. Brockmeyer, H. Harms, J. Loffler, H. Reincke, R. Schmidt, B. Stachel, W. von Tumpling, A. Wanke, Pharmaceuticals in the river Elbe and its tributaries, Chemosphere 57 (2004) 107-126;

(b) Y. Zhang, S. U. Geissen, C. Gal, Carbamazepine and diclofenac: Removal in wastewater treatment plants and occurrence in water bodies, Chemosphere 73 (2008) 1151-1161.

[25] Directive 2013/39/UE of the European Parliament and the Council of the 12 August 2013 amending Directive 2000/60/EC and 2005/105/EC regards priority substances in the field of water policy, Official J. Eu. Union 2013.

[26] L. H. Santos, A. N. Araújo, A. Fachini, A. Pena, C. Delerue-Matos, M. C. Montenegro Journal of Hazardous Materials, Ecotoxicological aspects related to the presence of pharmaceuticals in the aquatic environment, J. Hazard. Mater. 175 (2010) 45–95.

[27] (a) M. Cleuvers, Toxicol. Lett., Aquatic ecotoxicity of pharmaceuticals including the assessment of combination effects, Toxicol. Lett. 142 (2003) 185-194;

(b) M. Cleuvers, Ecotoxicol. Environ. Saf., Mixture toxicity of the anti-inflammatory drugs diclofenac, ibuprofen, naproxen, and acetylsalicylic acid, Ecotoxicol. Environ. Saf. 59 (2004) 309-315.

[28] O. Monticelli, A. Bottino, I. Scandale, G. Capannelli, S. Russo, Preparation and properties of polysulfone-clay composite membranes, J. Appl. Polym. Sci., 103 (2007) 3637-3644.

[29] Lee, C., Wei, X., Li, Q., Carpick, R., Kysar, J. W., Hone, J., 2009. Elastic and frictional properties of graphene. Phys. Status Solidi B 246, 2562-2567.

[30] J. W. Suk, R. D. Piner, J. An, R. S. Ruoff, Mechanical properties of monolayer graphene oxide, ACS Nano 4 (2010) 6557-6564.

[31] V. Palermo, I. A. Kinloch, S. Ligi, N. M. Pugno, Nanoscale Mechanics of Graphene and Graphene Oxide in Composites: A Scientific and Technological Perspective. Adv. Mater. 28 (2016) 6232-6238.

[32] J. Han, N. M. Pugno, S. Ryu, Nanoindentation cannot accurately predict the tensile strength of graphene or other 2D materials, Nanoscale, 7 (2015) 15672-15679.

[33] A. Liscio, K. Kouroupis-Agalou, X. Diez Betriu, A. Kovtun, E. Treossi, N. M. Pugno, G. De Luca, L. Giorgini, V. Palermo, Evolution of the size and shape of 2D nanosheets during ultrasonic fragmentation, 2D Materials, 4 (2017) 025017.

[34] A. Pobudkowska, U. Domanska, Study of Ph-dependent drugs solubility in water. Chem. Ind. Chem. Eng. Q. 20 (2014) 115-126.

[35] (a) J. Eastoe, J. S. Dalton, Dynamic surface tension and adsorption mechanisms of surfactants at the air–water interface. Advances in Colloid and Interface Science 85 (2000) 103-144. (b) J. J. Skopp, Derivation of the Freundlich Adsorption Isotherm from Kinetics, Chem. Educ. 86 (2009) 1341-1343.

[36] M.M. Dubinin, E.D. Zaverina, L.V. Radushkevich, Sorption and structure of active carbons. I. Adsorption of organic vapors, *Zh. Fiz. Khim.* 21 (1947) 1351-1362.

[37] A. Jain, R. Balasubramanian, M. P. Srinivasan, Production of high surface area mesoporous activated carbons from waste biomass using hydrogen peroxide-mediated hydrothermal treatment for adsorption applications. Chem. Eng J. 273 (2015) 622-629;

[38] Z. Geng, Y. Lin, X. Yu, Q. Shen, L. Ma, Z. Li, N. Pan, X. Wang, Highly efficient dye adsorption and removal: a functional hybrid of reduced graphene oxide-Fe3O4 nanoparticles as an easily regenerative adsorbent J. Mater. Chem. 22 (2012) 3527-3535.

[39] Z. Zou, Y. Zhang, H. Zhang, C. Jiang, A combined H3PO4 activation and boron templating process for easy synthesis of highly porous, spherical activated carbons as a superior adsorbent for rhodamine B, RSC Adv. 6 (2016) 15226-15233.

[40] H. Sun, L. Cao, J. Liu, Magnetite/reduced graphene oxide nanocomposites: One step solvothermal synthesis and use as a novel platform for removal of dye pollutants, Nano Res. 4 (2011) 550-562.